Conduction cooled narrow linewidth sub-nanosecond multi-beam laser*

CHENG Yong (程勇), **TAN Chaoyong** (谭朝勇)**, **LIU Xu** (刘旭), **CHEN Xia** (陈霞), **ZHU Mengzhen** (朱孟真), **and WEI Jingsong** (魏靖松)

Ordnance NCO Academy, Army Engineering University, Wuhan 430075, China

(Received 27 October 2020; Revised 17 December 2020)

A conduction cooled high peak power, narrow linewidth, and sub-nanosecond multi-beam laser as an excellent candidate for non-scanning lidar is demonstrated. This laser is based on master oscillator power amplifier (MOPA) scheme which consists of a pulse pumped Nd:YAG/Cr^{4+}:YAG microchip laser as the master oscillator and a high efficient grazing incidence Nd:YVO_4 slab amplifier, and the output beam is expanded to 100 mm diameter by a 50× low aberration Galileo beam expander and then divided into a 50×2 staggered arrangement multi-beam array by a diffractive laser splitter. The laser operates at 1 064.28 nm with a spectral linewidth about 20 pm, which generates 1 mJ, 0.78 ns pulses at 7 kHz rate. The fluctuation of output power is less than ±2% when it works continuously for 1 h. The energy uniformity of the 100 sub-beams is up to 90%, the divergence of each sub-beam is about 20 μrad, and the total transmission efficiency of the diffractive laser splitter is more than 85%.

Document code: A **Article ID:** 1673-1905(2021)09-0518-5

DOI https://doi.org/10.1007/s11801-021-0167-6

Multi-beam laser with some features, such as narrow linewidth (*FWHM*: tens of picometers), multi-kHz repetition, short pulse duration (<1 ns), high peak power intensity (>1 MW) and high stability, is one of the key components of non-scanning lidar systems[1-3].

There are multiple approaches to achieve single frequency, kHz repetition rate, sub-nanosecond pulses and near diffraction limited beam quality laser, but they almost use a master oscillator power amplifier (MOPA) scheme which consists of a high repetition, short pulse duration and near diffraction limited beam quality oscillator and high efficient laser amplifier.

Some remarkable approaches of such multi-kHz MOPA laser system with pulse duration <1 ns, pulse energy >1 mJ and narrow linewidth have been reported recently[4-7]. Xie Yin et al reported a conduction cooling and compact, high peak power, nanoseconds pulse laser. This laser is based on Nd:YAG microchip and Nd:YVO_4 slab amplifier, producing an output pulse energy of 2.3 mJ and pulse width of 1 ns while the oscillator provides 82 μJ pulse energy at 1 kHz[4]. Planar waveguide (PWG) power amplifier has also been proved to be an excellent power scaling approach[5]. Pumped by 90 W 940 nm diode laser, the highest amplified power reached 22 W (2.2 mJ at 10 kHz, 0.8 ns), the total electrical to optical efficiency was near 11%. The linewidth was about 0.02 nm, and the M2 of the output beam reached 1.1.

Recent studies have proved that MOPA system with side-pumped grazing incidence Nd:YVO_4 slab amplifier is an excellent solution to achieve high energy gains while preserving oscillator laser beam quality and emission spectrum[6-13]. A. Agnesi et al reported a grazing incidence amplifier generating 1—10 kHz, ~500 ps single longitudinal mode pulses with energy exceeding 500 μJ, the total energy extraction efficiency was 13%[6]. Sun et al reported an Nd:YVO_4 grazing incidence slab amplifier with average output power of 20.5 W at 20 kHz, pulse duration of 2.3 ns[10]. Tang and Xu et al reported such incidence amplifier Nd:YVO_4 slab laser amplifier with the pulse energy of 126 μJ at 100 kHz[11,12].

For multi-beam application, microlens, fiber optics, diffracted optical element (DOE) and liquid crystal spatial light modulator are the most commonly used devices for beam splitting[2,3,14-17]. The DOE is a diffractive beam splitter that generates multi-beam array from a single input beam, it is an elegant beam splitting approach for large number sub-beams because it is simple, efficient, and environmentally insensitive. Thus it is used in most applications.

In this letter, we present a multi-beam MOPA laser system. It consists of a low energy high repetition and single frequency master oscillator, a high efficient amplifier stage and a laser beam splitter module. The

* This work has been supported by the National Science and Technology Major Project of China (No.2014ZX01005-101-003), the National Natural Science Foundation of China (No.61705268), and the Science and Technology Innovation Project of Army Engineering University (No.KYWHJQZL2002).

** E-mail: tcyong@126.com

configuration of this multi-beam MOPA laser system is shown in Fig.1. The MOPA laser generates 20 pm spectral line width at 1 064.28 nm, 1 mJ/pulse, and 0.78 ns pulse duration at 7 kHz repetition rate. The output power instability reaches ±2% while the laser has operated continuously for 1 h. A laser beam splitter module with 100 mm output clear aperture is used to divide the single-beam profile into 50×2 sub-beam arrays. This module consists of a 50× low aberration Galileo beam expander and a custom built high precious DOE as the laser splitter. The divergence of the sub-beams is about 20 μrad and the energy uniformity of the sub-beams reaches 90%. This laser source is a valuable tool for application such as non-scanning mapping lidar.

In the MOPA laser, a Cr^{4+}:YAG passively Q-switched Nd:YAG laser is used as the master oscillator, and a simple compact, double-pass grazing incidence Nd:YVO_4 slab module is used as the amplification stage. The seed signal from the master oscillator is amplified in the grazing incidence Nd:YVO_4 amplifier in double-pass scheme. The amplified beam is then expanded by a 50× beam expander, and finally divided by a DOE (shown in the rigth of Fig.1) into 50×2 sub-beams.

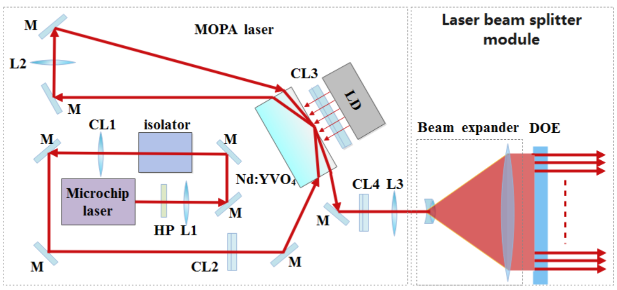

Nd:YVO_4: a-cut slab; HP: half wave plate; LD: laser diode; M: high reflectivity mirror; L1—L3: spherical lenses; CL1—CL4: cylindrical lenses

Fig.1 The setup of the multi-beam laser system

The prototype is shown in Fig.2. The right module in Fig.2 is the MOPA laser source, and the left is the integrated 50× laser beam expander and the custom-built DOE.

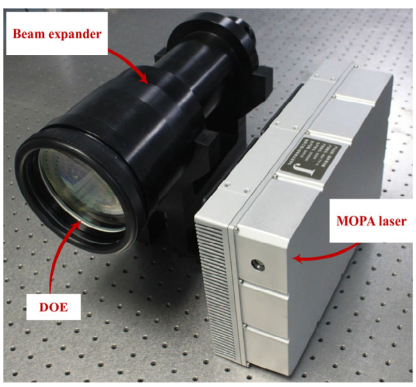

Fig.2 Prototype of the multi-beam laser

The passively Q-switched Nd:YAG/Cr^{4+}:YAG microchip laser is longitudinally pumped by a pulse driven laser diode. The Cr^{4+}:YAG unsaturated transmission and output coupling is properly set to achieve 3 μJ, 0.77 ns pulses (*FWHM*) at 7 kHz repetition (shown in Fig.3(a) and (b)). The spectral property is measured by optical spectrum analyzer AQ6370. While the wavelength resolution is set to be 0.02 nm, the highest resolution of AQ6370, the central wavelength is measured to locate at 1 064.28 nm and spectral width (*FWHM*) is about 0.02 nm (shown in Fig.3(c)), which means the actual value of spectral width may be even less than 0.02 nm. Diffraction limited mode operation is observed at the repetition rate of 7 kHz (shown in Fig.3(d)). The beam ellipticity is measured to be 0.96, and the beam quality is M_x^2=1.18, M_y^2=1.16.

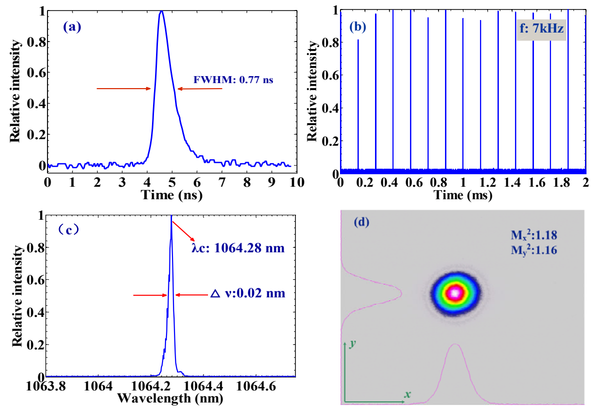

Fig.3 The output of the master oscillator: (a) The pulse duration; (b) The pulse repetition rate; (c) The output spectrum; (c) The output beam profile

The seed beam is reshaped by lenses and injected into an a-cut Nd:YVO_4 amplifier. A Farady magnetic-optic isolator is inserted between the microchip laser and the amplifier to avoid the feedback beam from the amplifier damaging the microchip laser.

The Nd:YVO_4 crystal used as the amplifier gain media is a 22 mm×5 mm×1.2 mm, 13° wedged slab. The Nd-doping level is 1% (atomic). The input and output faces of the slab are antireflection (AR) coated at 1 064 nm and the pumped face is AR coated at 808 nm. The two 22 mm×5 mm faces of the slab are welded to the copper heat sink by indium. The waste heat is transferred by a thermoelectric cooler (TEC), and the emission spectrum of the Nd:YVO_4 slab will not deviate as the temperature is well controlled. The slab is pumped by a TE polarized CS packaged laser diode (LD), the polarization of pump source is parallel to the c-axis of the Nd:YVO_4 slab, and the maximum pump power reaches 55 W at 808 nm (25 °C). The pump beam is collimated by a cylindrical lens (CL3 shown in Fig.1), yielding a vertical gain sheet of about 200 μm and horizontal gain area of about 10 mm. The polarization of the pump light is parallel to the *c*-axis of the slab. The LD is mounted on a copper heat sink. A TEC is used to control the temperature of LD. Both the Nd:YVO_4 slab and the LD are set to operate at 25 °C. The MOPA laser prototype shown in Fig.2 is air-cooled. The laser temperature control module is compact and simple in structure, and it can reduce the weight and operation complexity of the laser system.

As the fluorescence lifetime of Nd:YVO_4 is only 100 μs, to be compatible with the injected seed signal, the amplifier's pump diode is set to operate at 7 kHz and each pump pulse duration is 100 μs. In order to optimize the energy extraction in the Nd:YVO_4 slab amplifier, both the transverse mode and the polarization of the seed and pump beam should be well matched. As the seed beam is circular symmetrical Gaussian beam, to match the gain sheet dimension in the Nd:YVO_4 slab, a pair of cylindrical lenses (CL1 and CL2 shown in Fig.1) with different focuses are used to reshape the transverse seed spot along the vertical and horizontal axes. The grazing angle is also chosen to be as small as possible in order to maximize the gain while avoiding clipping effects. As the absorption property of Nd:YVO_4 crystal is polarization relevant[18], the polarization of the CS packaged LD is set parallel to the c-axis of the slab.

The Faraday magnetic-optic isolator shown in Fig.1 is necessary for MOPA operation. It is indispensable to prevent self-lasing and dangerous, high intensity back injections in the direction of the master oscillator. In the double-pass sketch, the backward propagating spontaneous emission originates at the output end of the amplifier may pass through the amplifier twice and be amplified sharply. Then at the output mirror of the master oscillator, parts of the amplified spontaneous emission (ASE) will reflect back into the amplifier and be quickly amplified along the single-pass and double-pass beam paths because of its extremely high gain, thus the effective energy extraction efficiency will be decreased. At the same time, the transmitted ASE at the output mirror will feed back into the microchip laser. This effect may increase the number of modes lasing in the microchip and significantly change the master oscillator's spectrum behavior, even damage the monoblock microchip crystal if the feedback power is too strong.

The total power of the seed injected into the amplifier is about 13 mW. The output power curve versus the pump power is shown in Fig.4. With 40 W diode pump power, a maximum of 2.4 W amplified output power at the pulse repetition of 7 kHz is achieved under single-pass amplification, maximum output power of 7.2 W is obtained after the double-pass amplification, that means the pulse energy reaches 1.03 mJ. The total energy extraction efficiency reaches 18%. Reliable operation of the laser has been proved by experiment. As shown in Fig.5, the output power instability is measured to be ±2% while the prototype has operated continuously for 1 h.

The spectrum of the double-pass amplifier is shown in Fig.6(a). When the pump power is below 40 W, the unwanted ASE is suppressed, and the pulse spectrum after amplification is significantly the same as that of the master oscillator. When the pump is larger than 40 W, the ASE grows quickly to an unacceptable level. When the pump power increased from 40 W to 55 W, the ASE also increases violently (the ASE spectrum shown in Fig.6(b)), the measured laser emission spectrum consists of two modes spaced about 0.2 nm apart. The signal spectrum still located at 1 064.28 nm and the *FWHM* remains about 0.02 nm, but the ASE emission is from about 1 064.05 nm to 1 064.1 nm. To suppress the ASE emission, the pump power should be limited to be no larger than 40 W.

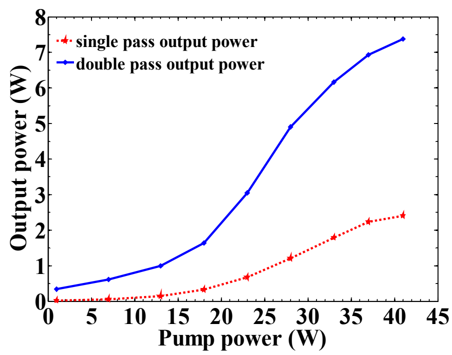

Fig.4 Output power vs. pump power for the single-pass and double-pass amplification

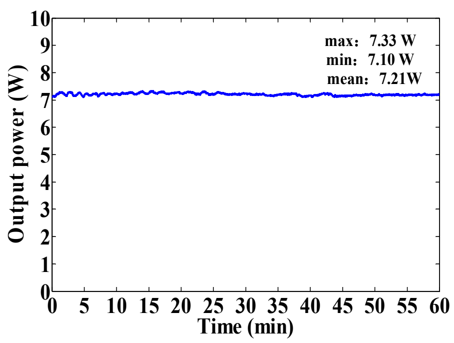

Fig.5 The output power curve of the prototype

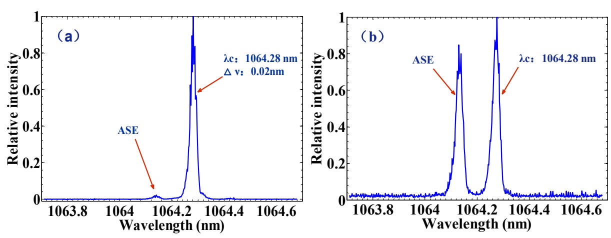

Fig.6 Output spectra of the double-pass amplifier: (a) 40 W pump power; (b) 55 W pump power

Temporal pulse shapes are shown in Fig.7. Pulse duration of the double-pass beam is about 0.78 ns at 7 kHz, the amplified pulse width is found to be almost the same as that of the oscillator. The total peak power is in exceed of 1.3 MW.

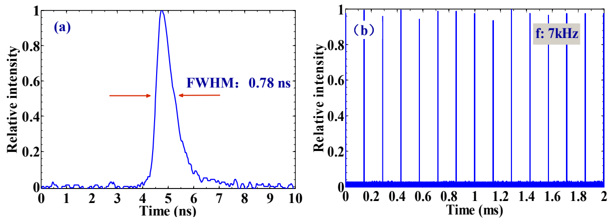

Fig.7 The output of the double-pass amplifier: (a) The pulse duration; (b) The pulse repetition rate

Due to the cylindrical lenses used for signal beam reshaping, the output beam after the double-pass amplifier is elliptical, not suitable for the latter beam expanding and splitting. A beam reshaping module consists of a cylindrical lens and a spherical lens is used to reshape the amplified beam into circular symmetrical Gaussian distribution. The reshaped beam is shown in Fig.8. Beam quality is well preserved. The beam ellipticity is measured to be 0.90, and the beam quality is measured to be M_x^2=1.51, M_y^2=1.43.

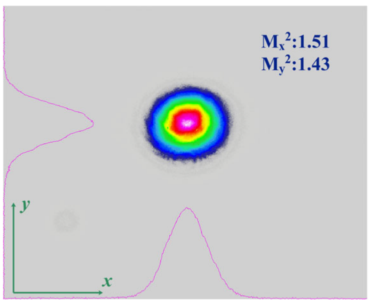

Fig.8 Output beam profile of the double-pass amplifier

The amplified beam is directed through a 50× low aberration Galileo beam expander and the beam diameter is then scaled-up to about 100 mm, with the divergence angle about 20 μrad. Then the beam propagates through the DOE laser splitter (shown in Fig.9). The far field profile is reshaped by the DOE into 50×2 beam array as shown in Fig.9. The far field distribution consists of two staggered arrangement rows beams, with each row of 50 sub-beams.

The customized DOE is the key device for beam splitting. Whether it can be used as the multi-beam array splitting depends on its specifications such as the diffraction efficiency and uniformity.

The 2D and 3D distributions in Fig.9 show that the 100 sub-beams arrange evenly, there is no redundant diffraction spot in the far field. Each sub-beam has a Gaussian intensity distribution and divergence angle is measured to be nearly the same, about 20 μrad. The angle between the optical axis of adjacent sub-beams in the same row and the angle between the two adjacent sub-beam rows are also about 40 μrad. Energy uniformity of all the 100 sub-beams is measured to be about 90%. The total transmit efficiency is more than 85%.

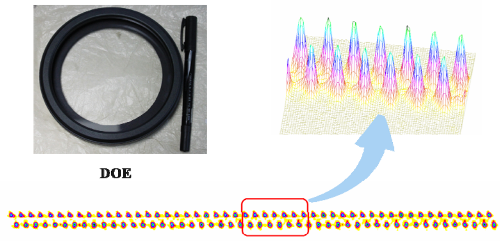

Fig.9 The OEM diffractive laser splitter and the final output profile

In conclusion, by using grazing incidence MOPA laser and laser beam splitter module, a high peak power, narrow linewidth, sub-nanosecond multi-beam laser is demonstrated. The MOPA laser consists of a monoblock Nd:YAG/Cr^{4+}:YAG microchip master oscillator, a grazing incidence double-pass Nd:YVO_4 slab amplifier, a 808 nm CS packaged LD pump source, in excess of 7 W output power has been demonstrated at frequency rate of 7 kHz, 0.78 ns pulse duration and 20 pm spectral width. The amplifier preserves the pulse duration, the beam quality and emission spectrum of the seed signal. The fluctuation of output power is below ±2% when the laser operates continuously for 1 h. The amplified beam size is scaled up by a 50× beam expander and at last split into a 50×2 beam array by a custom built DOE. The divergence of the sub-beams is about 20 μrad. The energy uniformity of the 100 sub-beams reaches 90%. It is also with potential for any other multi-beam reshaping by utilizing specific customized DOEs. This laser can be used as a component for future remote sensing applications such as high resolution non-scanning mapping lidar.

References

[1] Mark A. Stephen, Anthony W. Yu and Michael A. Krainak, Proc. SPIE **8154**, 815406 (2011).

[2] A.W. Yu, M.A. Krainak, D.J. Harding, J.B. Bshire and X. Sun, Proc. SPIE **8599**, 85990 (2013).

[3] Matthew McGill, Thorsten Markus, V. Stanley Scott and Thomas Neumann, Journal of Atmospheric and Oceanic Technology **30**, 345 (2013).

[4] Xie Yin, Meng Junqing, Zu Jifeng and Chen Weibiao, Chinese Journal of Lasers **42**, 0902005 (2015). (in Chinese)

[5] Anthony W. Yu, Alexander Betin, Michael A. Krainak, Derek Hendry, Billie Hendry and Carlos Sotelo, Highly Efficient Yb:YAG Master Oscillator Power Amplifier Laser Transmitter for Future Space Flight Missions, 2012 Conference on Lasers and Electro-Optics, 2012.

[6] A. Agnesi, P. Dallocchio, F. Pirzio and G. Reali, AppliedPhysics B **98**, 737 (2010).

[7] J. Morgenweg and K. S. E. Eikema, Optical Letters **37**, 208 (2012).

[8] Takaharu Yoshino, Hiroki Seki, Yu Tokizane, Katsuhiko Miyamoto and Takashige Omatsu, Journal of the Optical Society of America B **30**, 894 (2013).

[9] Yu Zhenzhen, Hou Xia, Zhou Qunli, Zhou Cuiyun and

Wang Zhijun, Chinese Journal of Lasers **40**, 0602003 (2013). (in Chinese)

[10] Zhe Sun, Qiang Li, Yongling Hui, Menghua Jiang and Hong Lei, Proc. SPIE **9449**, 94491G (2014).

[11] Tang Chao, Xu Shuangfu, Zhang Xiang, Wang Yong, Liu Bin, Liu Dong, Xiang Zhen, Ye Zhibin and Liu Chong, Chinese Journal of Lasers **44**, 1201003 (2017). (in Chinese)

[12] S. Xu, C. Tang, Y. Wang, F. Zheng, Z. Xiang, D. Liu, X. Zhang, Z. Ye and C. Liu, Chinese Journal of Lasers **45**, 0101008 (2018). (in Chinese)

[13] Hui YongLing, Jiang MengHua, Lei Hong and Li Qiang, Applied Laser **39**, 490 (2019).

[14] Luis Ramos-Izquierdo, V. Stanley Scott III, Joseph Connelly, Stephen Schmidt, William Mamakos, Jeffrey Guzek, Carlton Peters, Peter Liiva, Michael Rodriguez, John Cavanaugh and Haris Riris, Applied Optics **48**, 3035 (2009).

[15] Shu Rong, Li Ming, Huang Genghua and Hou Libing, Design and Performance of a Fiber Array Coupled Multi-Channel Photon Counting, 3D imaging, Airborne Simulator for Lidar System, China High Resolution Earth Observation Conference, 2014.

[16] Li Ming, Hou Jia, Zhou Chenglin and Shu Rong, Infrared and Laser Engineering **46**, 0730001 (2017). (in Chinese)

[17] Liu Bo, Zhao Juanying, Sui Xiaolin, Cao Changdong, Yan Ziheng and Wu Ziyan, Infrared and Laser Engineering **48**, 0606001 (2019). (in Chinese)

[18] Chen Sanbin, Zhou Shouhuan, Tang Xiaojun, Liu Yang and Guo Lina, Infrared and Laser Engineering **39 supplement**, 97 (2010). (in Chinese)